

Charge dissociation at an organic-organic interface: The role of the environment

Shane R. Yost and Troy Van Voorhis

Massachusetts Institute of Technology, Cambridge, MA 02139

Introduction

Organic semiconductors (OSCs) are used in devices such as organic light emitting diodes (OLEDs) and organic photovoltaics (OPVs). These devices derive their functionality from at least one interface between two OSC materials; this is where excitons are converted into charge transfer (CT) states or vice versa, caused by the offset in the HOMO and LUMO energy levels of the different molecules¹. The electrostatic environment near this interface can be dramatically different from the bulk due to the different packing and polarization of the two molecular layers, leading to effects like interface dipoles and band bending. These phenomena can have a profound influence on carrier generation and loss mechanisms in OPVs and OLEDs, but the underlying physical chemistry is as yet poorly understood.

Given the localized nature of the different states in OSCs, one expects a combined quantum mechanical/molecular mechanical (QM/MM) scheme to give a faithful description of the organic-organic interface. Indeed, we have successfully used QM/MM to model a crystalline OSC (Alq₃)², yielding quantitative predictions for both transport and optical properties. In this study, we use the QM/MM framework to gain further insight into the energetics at the organic-organic interface. Hence, in our study we simulate the interface between two molecules that have been individually well characterized: metal-free phthalocyanine (H₂Pc) and 3,4,9,10-perylenetetracarboxylic bisbenzimidazole (PTCBI).

Using the QM/MM model, we obtained an atomistic picture of the H₂Pc/PTCBI interface which reproduces the necessary energy level orderings for a functioning OPV device. Near the interface we find shifted values in the IP and EA, showing that band bending effects at the interface *must* be included to accurately estimate the binding energies of the interfacial CT states. Further, the CT binding energy shows sensitivity to the relative molecular orientations and thermal fluctuations, highlighting the influence of disorder on the energy landscape. Importantly, the combination of band bending effects and fluctuations in CT binding energies make it possible for relaxed CT states to dissociate into free carriers *with no barrier*. This finding improves our understanding of exciton dissociation and carrier generation mechanisms in OPVs, which is a subject of much current interest. The results further show that designing an interface where charges are less solvated due to poor packing between the two molecules can increase the charge separation.

Computational Details

Our study can be divided into 1) calculations performed on bulk H₂Pc and PTCBI systems and 2) calculations performed on the H₂Pc/PTCBI interface; this allows us to benchmark our calculations by comparing to experimental measurements on single crystals and also examine effects of the interface by comparing bulk and interface calculations. Each study began with a pure NVT MM dynamics simulation, where the simulation cell contained several hundred molecules that are treated classically (Figure 1 left). Several snapshots were harvested from this MM dynamics trajectory. In a given snapshot, a select few molecules were chosen to be treated quantum mechanically while interacting with the MM environment (Figure 1 right). QM/MM single-point calculations were then performed, and repeated over many snapshots to obtain ensemble

averaged values of material properties. We refer the reader to our previous work² for simulation details including the form of the MM force field, and the method used to construct the parameters.

Interface Structure For construction of the MM systems we started with a pure 14X7X5 (3X14X5) supercell of the experimental crystal structure for a total of 490 (420) PTCBI (H₂Pc) molecules. The H₂Pc/PTCBI interface was constructed by aligning the (001) and (010) crystal faces of the H₂Pc and PTCBI supercells along *z*; periodic boundary conditions were applied along *x* and *y* (i.e. perpendicular to the interface), and the system was relaxed under constant pressure (1 bar and 300K) for 1 ns. All three systems were evolved under NVT dynamics for 5 ns at 300 K. The final 4 ns of the constant-volume dynamics were sampled at 40 ps intervals to obtain 100 snapshots for QM/MM calculations.

Density Functional Calculations. All of the QM/MM calculations were done using the CHARMM-Q-Chem interface, and all pure MM calculations were run in Gromacs 4.0. All quantum calculations were performed with Q-Chem 3.2 using the PBE0 functional and 6-31G* basis set. The charge transfer states were obtained using constrained DFT on two molecules with an extra electron placed on PTCBI and one electron removed from H₂Pc.

Results and Discussion

We start by computing the band offset of bulk H₂Pc and PTCBI, given in Table 1. The transport gap (TG) is given by the difference in the ionization potential (IP) of H₂Pc and the electron affinity (EA) in PTCBI. Here we note that the TGs and band offset, the more critical quantities for device performance, are in good agreement with experimental values despite larger errors in the IPs and EAs themselves. This is because there are roughly equal shifts in the IP and EA when increasing the basis set (+0.2 eV with 6-311G*) and when placing a molecule in the electrostatic environment of the crystal (-0.3 eV).

Organic-Organic Interface. We sample five crystallographically distinct nearest-neighbor CT pairs at the interface and compute the CT binding energy (BE, given by $E_{BE}=E_{TG}-E_{CT}$). Using the procedure provided in Ref 3, we fit the inverse of the BE to a linear combination of intermolecular distances; our results are shown in Figure 2. This choice of a linear combination of intermolecular distances for the coordinate in Figure 2 is made to filter out the relative molecular orientation as much as possible. The BE has a clear R^{-1} decay as a function of distance, arising from the Coulomb interaction between the electron on the acceptor and the hole on the donor; however, this trend was not observed when center-of-mass distances were used, highlighting the important orientational dependence for these planar molecules. There is a clear scatter of 0.1 eV on top of the Coulombic decay which we attribute to thermal fluctuations. From moment to moment, the CT energy of a given dimer will fluctuate by a few kT . Thus, at any instant there can easily be a more distant CT pair that has a lower energy than a compact pair due to random fluctuations in molecular orientation. These variations are expected to aid the initial charge separation at the organic-organic interface.

Perhaps surprisingly, the average energy of the CT states (~1.6 eV) is higher than the bulk band offset (1.5 eV), giving an apparent CT binding energy of -0.1 eV; that is to say, the CT states seem to be unbound! We find that this can be explained by the significant contribution of interface effects to the band offset. In Figure 3 we plot the IP and EA of H₂Pc/PTCBI vs. the distance from the interface. The EA of PTCBI (IP of H₂Pc) decreases (increases) as one moves toward the interface by 0.1 (0.15) eV, such that the band offset at the interface is 0.25 eV larger the bulk value and giving an average CT binding energy of ~0.15 eV. Thus the CT states are *locally* bound;

the energy of the electron-hole pair at the interface is more stable than a single electron plus a single hole at the same site. At the same time, the CT states are *globally* unbound; the electron and hole gain energy by migrating away from the interface.

The 'gap bending' effect at the OSC donor-acceptor interface has been previously calculated in different systems and with different models⁴. Our calculations did not find a significant dipole at the H₂Pc/PTCBI interface; instead, the gap bending appears to be due to differences in the polarizability and crystal packing. The interface has a stabilizing (destabilizing) effect on carriers in H₂Pc (PTCBI) because PTCBI has a higher dielectric constant than H₂Pc, and the relatively sparse packing introduces an overall destabilizing effect; our QM/MM simulations with a polarizable MM model were uniquely able to capture these effects^{Difley2010}.

There is much discussion in the literature on understanding the origins of the high internal quantum efficiency in OPVs and why the separation of a CT state appears to be essentially barrierless⁵. One prominent view is that the excess energy from exciton dissociation creates a "hot" CT state with sufficient kinetic energy to break free of the binding energy before thermal relaxation takes place⁶. Our work indicates different model which suggests that thermally relaxed CT states can break up easily due to competition between the decreased dielectric screening at the interface and the Coulomb attraction, the first increasing and the second decreasing the CT energy. For our current H₂Pc /PTCBI model system, the decrease in dielectric screening is larger than the Coulomb attraction, and thus there is little to no energy barrier for CT separation.

Conclusion

In this study we used a QM/MM model to investigate the H₂Pc /PTCBI donor-acceptor interface and obtained thermal distributions of the IP, EA, and CT energies. We obtained an accurate prediction of the band offset for this interface. We also find a strong dependence of the BE on the relative orientation of the molecules forming the CT pair. Showing that one route to decrease charge recombination is to design a system with planar molecules that at the interface are stacked as near to edge-to-edge as possible in order to decrease the CT binding energy. We addressed two effects on the CT state energy that depend on proximity to the interface: the electrostatic changes at the interface cause the band offset to increase by 0.25 eV, and the CT binding energy is strongest at the interface with a typical value of 0.15 eV. The competition between two effects create a situation where thermally relaxed CT states at the interface can easily separate into free carriers. In our model system, charge separation is downhill by about 0.1 eV.

Acknowledgement. This work is supported by the U.S. Department of Energy under DE-FG02-07ER46474

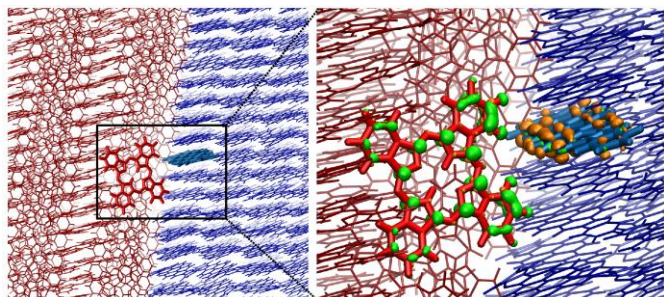


Figure 1. Illustration of the QM/MM method. Left: Disordered cell of the H₂Pc/PTCBI system described by MM. Center: Selection of a H₂Pc and PTCBI pair at the interface for calculation of the CT state energy.

Table 1. Calculated transport properties for H₂Pc and PTCBI. Experimental values, taken from Refs. 7,8, and 9, are given in parentheses. All values are reported in eV; computed values have a statistical uncertainty of ≤ 0.07 eV

| Material | IP | EA | TG | Band Offset |
|-------------------|------------|------------|------------|-------------|
| H ₂ Pc | 4.74 (5.2) | 2.43 (3.0) | 2.31 (2.2) | 1.54 (1.6) |
| PTCBI | 5.53 (6.2) | 3.20 (3.6) | 2.33 (2.6) | |

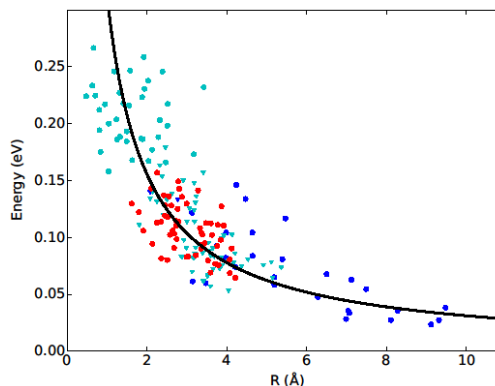


Figure 2. Plot of the distance dependence of the PTCBI/H₂Pc CT state binding energies. The coordinate R is a linear combination of intermolecular distances. Each different color/shape combination represents distinct dimer pairs in the simulation cell.

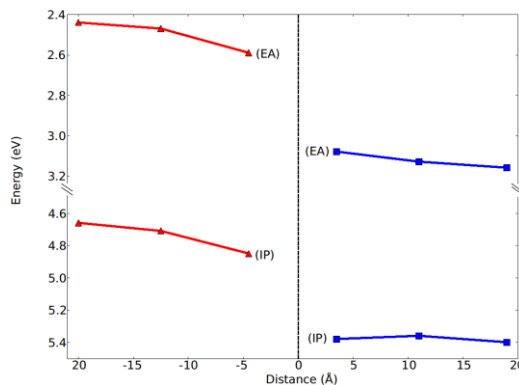


Figure 3. Plot of the average IP and EA of H₂Pc (red) and PTCBI (blue) crystal planes as a function of their distance from the interface. Each point has a standard deviation of about 50 meV.

References

- (1) Brédas, J.-L.; Norton, J.E.; Cornil, J.; Coropceanu, V. *Acc. Chem. Res.* **2009**, *42*, 1691-1699.
- (2) Difley, S.; Wang, L.-P.; Yeganeh, S.; Yost, S. R.; Van Voorhis, T. *Acc. Chem. Res.* **2010**, *43*, 995-1004.
- (3) Mahata, K.; Mahata, P. Maximizing Correlation for Supervised Classification. *Proceedings of the 2007 15th International Conference on Digital Signal Processing*, 2007; pp 107-110.
- (4) Verlaak, S.; Beljonne, D.; Cheyns, D.; Rolin, C.; Linares, M.; Castet, F.; Cornil, J.; Hermans, P. *Adv. Funct. Mater.* **2009**, *19*, 3809-3814.
- (5) Pensack, R. D.; Asbury, J. B. *J. Am. Chem. Soc.* **2009**, *131*, 15986.
- (6) Clarke, T. M.; Ballantyne, A. M.; Nelson, J.; Bradley, D. D. C.; Durrant, J. R. *Adv. Funct. Mater.* **2008**, *18*, 4029-4035.
- (7) Pope, M. *J. Chem. Phys.* **1962**, *36*, 2810.
- (8) Zahn, D.; Gavrilu, G.; Gorgoi, M. *Chem. Phys.* **2006**, *325*, 99-112
- (9) Rand, B. P.; Gence, J.; Heremans, P.; Poortmans, J. *Prog. Photovoltaics Res. Appl.* **2007**, *15*, 659-676.